Max Weiner
max.weiner@imf.tu-freiberg.de
Conceptualization, Methodology, Software, Formal analysis, Validation, Investigation, Writing - Original Draft
Institute of Metals Forming, TU Bergakademie Freiberg

Christoph Renzing
christoph.renzing@imf.tu-freiberg.de
Conceptualization, Methodology, Software, Formal analysis, Validation, Investigation, Project administration, Writing - Original Draft
Institute of Metals Forming, TU Bergakademie Freiberg

Matthias Schmidtchen
matthias.schmidtchen@imf.tu-freiberg.de
Conceptualization, Supervision, Resources, Project administration, Writing - Review & Editing
Institute of Metals Forming, TU Bergakademie Freiberg

Ulrich Prahl
ulrich.prahl@imf.tu-freiberg.de
Supervision, Resources, Writing - Review & Editing
Institute of Metals Forming, TU Bergakademie Freiberg

Funding
Not applicable.

Data Availability
Data openly available in a public repository that does not issue DOIs. Source code and data are available on GitHub at the following URLs:

Project Home `https://github.com/pyroll-project`

Core Package `https://github.com/pyroll-project/pyroll-core`

Benchmark Input and Data `https://github.com/pyroll-project/pyroll-pub1-benchmark`

Conflicts of Interest
The authors declare no conflicts of interest.

Acknowledgements
The authors thank Richard Pfeifer and Lukas Göschel for the preparation of the data.

Keywords
Rolling Simulation; Open Source; Groove Rolling

Rolling Process Variation Estimation Using a Monte-Carlo Method

M. Weiner * C. Renzing M. Schmidtchen U. Prahl

July 31, 2024

Industrial processes are subject to uncertainties originating in variations of input material and process parameters, especially if manual treatment is involved. For hot rolling processes, in particular, variations in workpiece geometry and temperature are affecting the final product shape and material properties. In this work, a Monte-Carlo-Method is applied to a fast hot rolling model based on the open-source rolling simulation framework PyRolL for estimating and analysing the variational behaviour of an experimental semi-continuous rolling line for steel wire production. The effects of input tolerances and manual transport between the reversing passes on the final product properties are quantified. Crucial stages of the process in regard to product properties are identified The findings are compared with practical knowledge and experimental results of statistical rolling trials.

1 Introduction

All technical processes are subject to certain variations. Knowledge and control of these variations is crucial for process stability and product quality. Sources of variations in a process are the variations already present in the input workpiece and newly generated variations due to imperfections of the process itself. In the case of wire and bar hot rolling industry regarded here, not only the product geometry, but also the final material properties sre highly sensitiv to the process conditions. Especially the temperature evolution of the workpiece within the rolling line has high impact on the microstructural transformation processes happening before, during and after forming. The product's microstructural state determines the mechanical properties and therefore its behavior in further processing and application. Current alloy concepts in the steel industry increase this problem, as the process window gets more narrow to achieve the property requirements for high-tech applications. The controlled combination of forming and thermally activated material transformation is commonly subsumed under the term thermo-mechanical treatment.

The classic way of analysing variational behavior with mathematical tooling is the error propagation using first order Taylor series expansions (see f.e. [1]). This concept is widely used in science and industry, especially to determine the error of indirect measurement processes. This procedure has two main problems. First, one needs to determine the first derivatives of the regarded function in each dimension, either analytically or numerically, which is rather problematic

*Corresponding author

if the function is complicated. Second, the error is commonly represented in terms of the variance, so there is only information about the spread, but not about the shape of the distribution inherent.

The usage of a Monte-Carlo Method circumvents these problems, and shall be proposed with this work. The term Monte Carlo Method (MCM) generally refers to a class of methods, which are characterized by the use of random numbers. These methods are rather diverse and serve different purposes. Here, the term shall be used for the concept of drawing random numbers as input for a function and analysing the results of several evaluations of this function, with different random inputs, with statistical methods. A detailed overview on this type of Monte Carlo methods is given by Lemieux [2]. The nature of the function can be complicated, even of a black-box type, where nothing about the internals of the function is known but the input and output interfaces. In this case, Monte Carlo methods can provide valuable information about the behavior of the function while altering inputs. Also, the complete distribution of the input variables is included in the estimation and is reflected in the results.

Here, the function equals the simulation procedure, so it is generally known, but complicated. For example, it is generally not possible, to compute derivatives of the outputs in dependence on the inputs in an analytical way. Even numerical derivation is hard, due to the multi-dimensional nature of most natural or technical systems and the pronounced non-linear behavior of the function.

The use of Monte Carlo methods for the analysis of variations in technical processes was reported before in the field of assembly of complicated structures, like in mechanical engineering and building construction (f.e. [3, 4, 5, 6, 7, 8]). However, in the field of rolling processes, there was no such attempt yet to the knowledge of the authors. The authors have previously used a similar approach to model powder morphology influences in sintering processes [9, 10]. The current work shall show the possibility of the application of Monte Carlo methods for the analysis of process variations in rolling processes. The focus lies hereby on the estimation of the workpiece temperature evolution and its impact on the microstructure state of the final product. The influence of variations in the initial workpiece and within the regarded process route is analysed and evaluated. Due to the need of a large number of function evaluations (simulation runs), the evaluation speed of the process model is crucial to the applicability of this approach.

Rolling simulation is currently dominated by the use of finite element (FE) based models. These are offering high accuracy and high resolution results at the expense of high computational resource usage. So these methods are inconvenient for the current need. Therefore, one-dimensional approaches shall be used here. These offer less accuracy and limited resolution, but are computable within fractions of seconds on typical personal computer systems. The current work is based on the open-source rolling simulation framework PyRolL [**pyroll2**], developed by the authors, which is a fast, open and flexible software package mainly aimed at groove rolling in reduction passes. The models used for the different parts of the problem can be exchanged and extended with low effort to the users needs.

2 Methods

2.1 Experimental Procedure

The object of the current investigation is the operation of the experimental semi-continuous rolling plant located at the Institute of Metal Forming, TU Bergakademie Freiberg. It consists of a two-high reversing roughing stand and four continuous finishing stands. The pass schedule of the current work consists of 10 oval-round reversing passes followed by 4 oval-round continuous

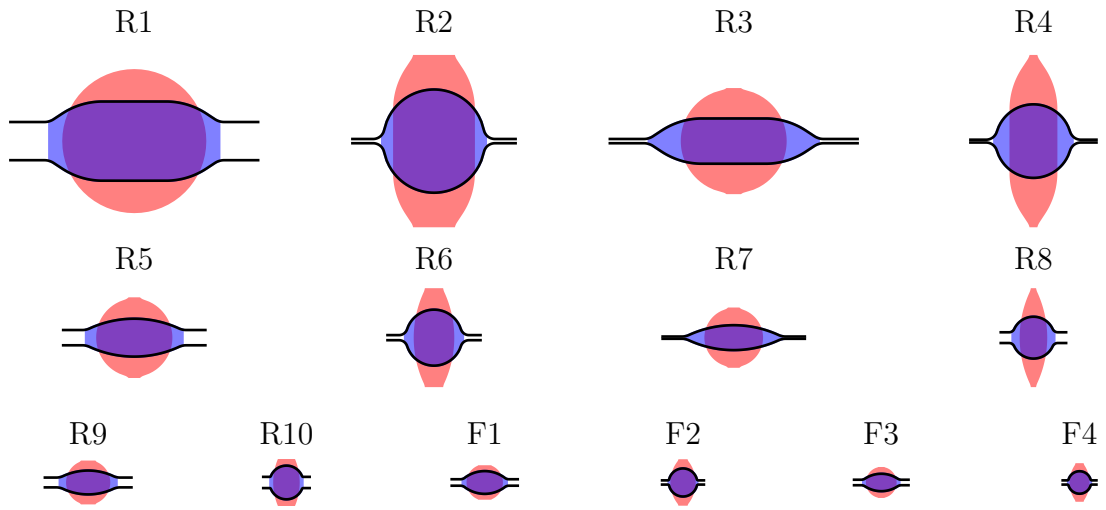

Figure 1: True Scaled Illustration of the Investigated Pass Sequence

finishing passes. A 50 mm round workpiece made of C45 carbon steel is rolled down to 8 mm diameter, starting at 1150 °C, resp. 1423.15 K. Details of the schedule are provided in Table 1 and in the supplemental material [11]. The profile shapes appearing in the schedule are illustrated in Figure 1.

Online measurements of the process conditions and workpiece state are done regarding roll force and torque, as well as workpiece temperature. The latter is measured using pyrometers at several points in the plant: at entry and exit of the reversing stand and before, between and after the finishing stands. The sensor signals are collected as timelines, so that they can be automatically analysed afterwards as described in subsection 2.3.

To achieve statistical certainty, a number of 45 rolling trials were carried out. This enables an estimation of the variations appearing. A major source of variation in these trials is the manual feeding of the workpiece into the reversing passes. The duration of those is scheduled with about 6 seconds. The actual time needed has to be investigated in this work, see subsection 2.3 for details.

2.2 Monte-Carlo Approach

The basic idea of the approach shown here is to simulate the rolling process several times with different input values, which are drawn by a random number generator according to predefined statistical distributions. Afterwards, the distribution of the results can be analysed by classic methods of descriptive statistics to obtain information about the process' variational behavior. The principle is shown in Figure 2.

This approach provides information about the overall variational behavior of the process. If a single source of variation is introduced in the input, the reaction of the process on this variable can be analysed. The count of variation sources introduced is generally unbounded. In contrast to classic Taylor series error propagation, the computational effort does not directly increase remarkably with increasing count of investigated parameters. However, an increase in sample size can be necessary to achieve sufficient certainty. The key problem is to obtain data describing the variations of the input variables. The tracing back of result variations to the input can be

Table 1: Principal Data of the Investigated Pass Sequence

#	Type	w mm	h mm	s mm	R_W mm	v $m\,s^{-1}$
R1	swedish oval	60.0	28.0	13.5	160.5	1.0
R2	round	36.6	36.5	1.5	160.5	1.0
R3	swedish oval	60.0	16.0	1.5	160.5	2.0
R4	round	27.6	26.0	1.0	160.5	2.0
R5	circular oval	34.0	13.4	5.4	160.5	2.0
R6	round	20.4	19.8	1.8	160.5	2.0
R7	circular oval	34.0	8.8	0.8	160.5	2.0
R8	round	14.7	14.8	3.8	160.5	2.0
R9	circular oval	20.1	8.5	3.5	160.5	2.0
R10	round	11.3	12.0	4.0	160.5	2.0
F1	circular oval	15.6	8.1	2.3	107.5	7.9
F2	round	10.1	10.0	1.5	107.5	9.3
F3	circular oval	12.8	6.2	2.0	107.5	12.1
F4	round	8.1	8.0	1.5	85.0	15.8

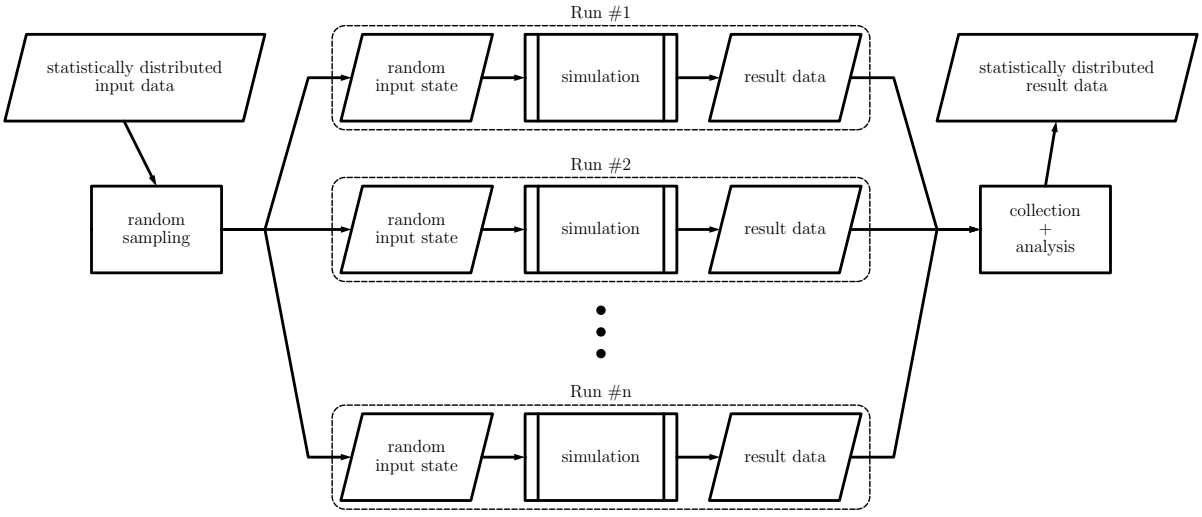

Figure 2: Chart of the Concept of Variation Estimation Using Monte Carlo Techniques

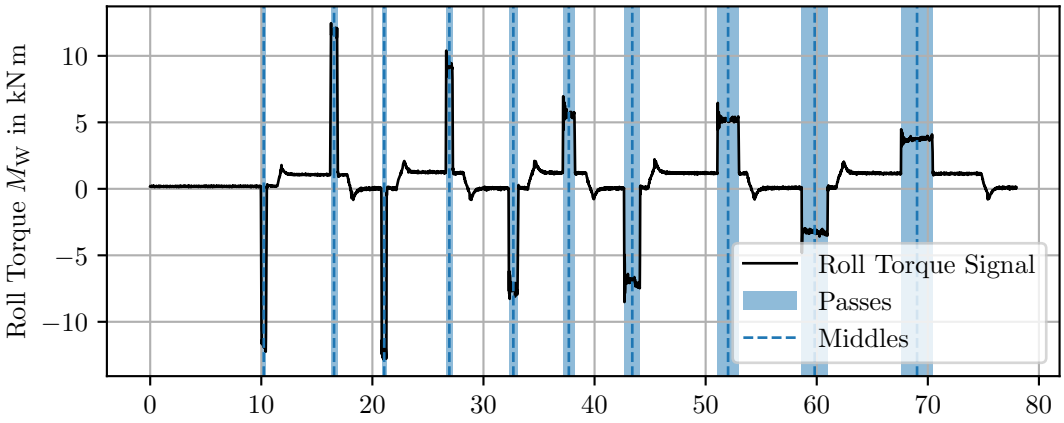

Figure 3: Example Roll Torque Signal With Automatically Determined Roll Pass Locations

done using classic correlation methods of descriptive statistics, however, with the same typical caveats. The main benefit of the approach is, that no information about the internals of the simulation procedure is needed for variational analysis, especially there is no need for derivatives of result values in dependence on the input. The simulation procedure can generally be treated as black box with defined input and output interfaces.

2.3 Statistical Data Acquisition

As input for the Monte-Carlo approach statistical descriptions of the regarded input variables are needed. Regarding the geometric variations of the input workpiece, the diameter of the samples was determined at multiple spots using a calibre. The initial temperature of the samples was determined using the pyrometer installed near the roll gap entry. Both were approximated using a normal distribution for sampling of random input values.

The question of varying inter-pass durations is crucial for scientific experiments on microstructure evolution, but currently often neglected. Mostly, only fixed durations between the reversing passes are included in the design calculations. Due to manual transport and feed of the workpiece to the following roll pass, the scheduled inter-pass durations are never realized in practice. Although, these deviations from the schedule influence the microstructure evolution of the sample, as well as the actual conditions in the roll passes. The current approach is aimed to help quantifying these deviations.

To obtain the inter-pass durations Δt_P from the timeline data, the passes have to be identified automatically. This was done by analysing the roll torque signal as plotted in Figure 3. The original signal was first downsampled and smoothed. Then, a difference filter was applied and the peaks of the resulting signal were determined. These peaks denote start and end times of the roll passes, the middle time of those was used as time coordinate of the roll pass. The distances of those were used as the inter-pass durations.

For the approximative description of the durations' distribution, a Weibull distribution was used. The probability density function (PDF) of the Weibull distribution is defined as in Equation 1, where $\alpha > 0$ and $\beta > 0$ are the shape and scale parameters. The distribution function was fitted on the observed data using the least-squares method.

$$p\left(\Delta t_{\mathrm{P}}\right) = \frac{\alpha}{\beta}\left(\frac{\Delta t_{\mathrm{P}}}{\beta}\right)^{\alpha-1} \exp - \left(\frac{\Delta t_{\mathrm{P}}}{\beta}\right)^{\alpha} \tag{1}$$

2.4 Core Simulation Procedure

In the current work, the open-source rolling simulation framework PyRolL [12, 13] was used to simulate the rolling process. Generally, the shown approach can be used with every rolling simulation software available, since the procedure does not depend on any internals of the simulation. A fast simulation approach, however, is favourable, since the simulation has to be done several, up to hundreds of, times. The models used here are of one-dimensional type, thus, they lack of resolution in other directions as the rolling direction and provide only limited accuracy, but at the benefit of high solution speed. They typically combine empirical approaches with simplified analytical solutions. The simulation was done with the basic configuration of PyRolL, which includes the empirical roll force and torque model of Hensel and Spittel [14], an integral thermal model approach according to Hensel et al. [15], contact area estimation according to **Zouhar1960** and roll flattening according to Hitchcock and Trinks [16]. Spreading was simulated using the equivalent flat pass according to Lendl [17, 18, 19] in conjunction with the spreading equation of **Wusatowski1969**. Details of software construction and model equations are provided in the documentation of PyRolL [20].

The models most important for the following elaborations will be discussed in brief. The temperature change of the workpiece was calculated by an integral heat balance as proposed by Hensel et al. [15] and given in Equation 2.

$$\Delta T = \Delta T_{\mathrm{Convection}} + \Delta T_{\mathrm{Contact}} + \Delta T_{\varphi} + \Delta T_{\mathrm{Radiation}} \tag{2}$$

$\Delta T_{\mathrm{Convection}}$ is the temperature change by convective heat flows according to Equation 3 with $\alpha_{\mathrm{Convection}}$ as a heat transfer factor, T_{∞} as the environment temperature, T as the current workpiece temperature and Δt as the duration of the process step.

$$\Delta T_{\mathrm{Convection}} = \frac{\alpha_{\mathrm{Convection}} A_{\mathrm{S}}}{\varrho c_{\mathrm{p}} V}\left(T_{\infty} - T\right)\Delta t \tag{3}$$

$\Delta T_{\mathrm{Contact}}$ is the temperature change by contact to the rolls according to Equation 4 with $\alpha_{\mathrm{Contact}}$ as a heat transfer factor and T_{R} as the temperature of the rolls.

$$\Delta T_{\mathrm{Contact}} = \frac{\alpha_{\mathrm{Contact}} A_{\mathrm{Contact}}}{\varrho c_{\mathrm{p}} V}\left(T_{\mathrm{R}} - T\right)\Delta t \tag{4}$$

$\Delta T_{\mathrm{Radiation}}$ is the temperature change by radiation according to Equation 5 with ϵ_0 as the Stefan's and Boltzmann's constant and ϵ_{r} as the relative radiation coefficient of the gray radiator.

$$\Delta T_{\mathrm{Radiation}} = \frac{\epsilon_0 \epsilon_{\mathrm{r}} A_{\mathrm{S}}}{\varrho c_{\mathrm{p}} V}\left({T_{\infty}}^4 - T^4\right)\Delta t \tag{5}$$

ΔT_{φ} is the temperature change by deformation according to Equation 6 with k_{Wm} as the empirical deformation resistance and φ_{eq} as the equivalent plastic strain. Since the deformation resistance is used here instead of the flow stress, this term also includes approximately the heat generation by inner and outer friction.

$$\Delta T_{\varphi} = \frac{0.95 k_{\mathrm{Wm}} \varphi_{\mathrm{eq}}}{\varrho c_{\mathrm{p}}} \tag{6}$$

The deformation resistance was taken as proposed by Hensel and Spittel [14] and given in Equation 7.

$$\frac{k_{\mathrm{Wm}}}{k_{\mathrm{f_{eq}}}} = 0.9901 + 0.106\frac{A_{\mathrm{Contact}}}{A_{\mathrm{eq}}} + 0.0283\left(\frac{A_{\mathrm{Contact}}}{A_{\mathrm{eq}}}\right)^2 + 1.5718\exp\left[-2.4609\frac{A_{\mathrm{Contact}}}{A_{\mathrm{eq}}}\right] + 0.3117\exp\left[-15.625\left(\frac{A_{\mathrm{Contact}}}{A_{\mathrm{eq}}}\right)^2\right] \quad (7)$$

The pay regard on the microstructure influence of the thermal variation involved in the process, a JMAK based recrystallization model was used. The JMAK approach is named after Johnson and Mehl [21], Avrami [22, 23, 24] and Kolmogorov [25]. It has gained a large popularity in modelling kinetics of transformation processes. The literature regarding recrystallization modelled by JMAK approaches is rather diverse [26, 27, 28, 29, 30, 31, 32, 33, 34, 35, 36, 37, 38, 39, 40, 41, 42, 43]. There are many forms of how the parameters can be described for materials under different conditions regarding strain φ, strain rate $\dot{\varepsilon}$ and temperature T. The following forms try to generalize them into one for all three major mechanisms: dynamic, metadynamic and static recrystallization. The Zener-Holomon-parameter [44] is not applied here, since sometimes different activation energies are used therein for the distinct mechanisms, so the Arrhenius-term is explicitly used in each equation. These equations are implemented in the JMAK Recrystallization Plugin for PyRolL [45]

The recrystallized fraction X in dependence on time t is given as Avrami-term as Equation 8, with the empirical parameters k an n, as well as the reference time t_{ref} and critical time t_{cr}.

$$X(t) = 1 - \exp\left[k\left(\frac{t - t_{\mathrm{cr}}}{t_{\mathrm{ref}} - t_{\mathrm{cr}}}\right)^n\right] \quad (8)$$

The critical time t_{cr} is the incubation time of the recrystallization, thus the time, when the recrystallization starts. It is calculated by an empirical approach according to Equation 9 with the material dependent parameters a_i and the activation energy Q_a.

$$t_{\mathrm{cr}} = a_1 \cdot \varphi_{\mathrm{in}}^{a_2} \cdot \dot{\varphi}^{a_3} \cdot d_{\mathrm{in}}^{a_4} \cdot \exp\left[\frac{Q_a}{RT}\right] \quad (9)$$

The reference time t_{ref} is often chosen as the time of half recrystallization $t_{0.5}$, then k in Equation 8 equals $\ln\frac{1}{2}$. It is calculated by an empirical approach according to Equation 10 with the material dependent parameters b_i and the activation energy Q_b.

$$t_{\mathrm{ref}} = b_1 \cdot \varphi_{\mathrm{in}}^{b_2} \cdot \dot{\varphi}^{b_3} \cdot d_{\mathrm{in}}^{b_4} \cdot \exp\left[\frac{Q_b}{RT}\right] \quad (10)$$

The grain size d_{RX} of the newly recrystallized grains is given by a similar approach according to Equation 11 with the material-dependent parameters c_i and the activation energy Q_c.

$$d_{\mathrm{RX}} = c_1 \cdot \varphi_{\mathrm{in}}^{c_2} \cdot \dot{\varphi}^{c_3} \cdot d_{\mathrm{in}}^{c_4} \cdot \exp\left[\frac{Q_c}{RT}\right] \quad (11)$$

These equations include all approaches found in the cited references for static, dynamic and metadynamic recrystallization. Parameters can be set to zero, if the respective dependency is not needed or not investigated. For dynamic recrystallization, the time t if often substituted by

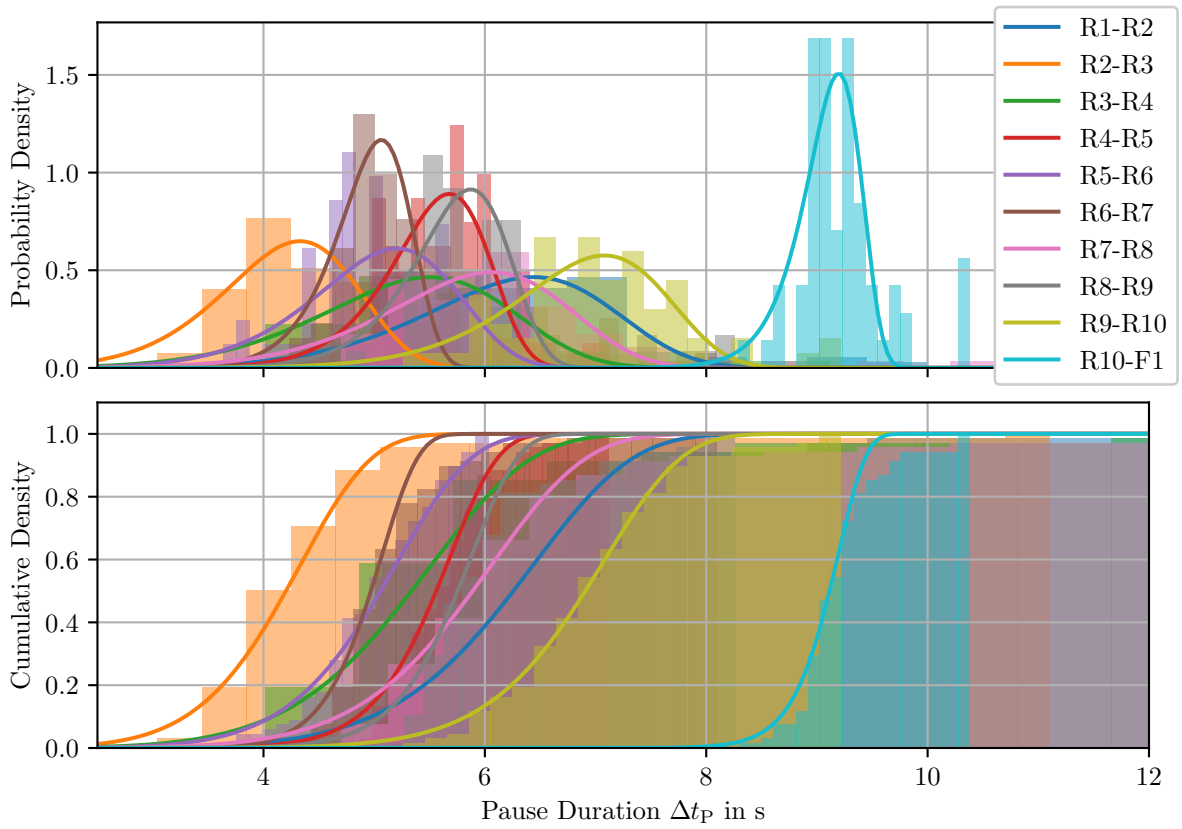

Figure 4: Density and Cumulative Histograms of Inter-Pass Durations With Fitted Weibull Distributions

the logarithmic strain φ under the assumption of constant strain rate, where the same empirical approaches are applied.

The material data and model coefficients used above were taken for the following simulations as in Table 2.

3 Results

3.1 Analysis of Inter-Pass Durations

Figure 4 shows the histograms of pause durations obtained from the torque signals with fitted Weibull distributions. The last pause (R10–F1) protrudes from the other distributions due to a technical difference, the workpiece is here fed into a driver which accelerates it to be fed into the first finishing pass. However, the other passes also do not form a unitary distribution. The distributions partially overlap, but there is no clear tendency remarkable. Therefore, it was decided to treat each pause distinctly with its own distribution function fit.

Table 3 shows the summary statistics of the distinct data sets alongside with the fitted beta-distribution parameters. The mean pause duration in most passes is slightly below the scheduled duration of 6 s. However, single events up to 21 s occur. The standard deviation is in the most passes below 1 s. The expectations of the fitted Weibull distribution function are constantly below the empirical means. The respective standard deviations are all far below the empirical ones.

Table 2: Material Data and Model Coefficients Used in the Simulations

(a) Flow Stress Model of C45 acc. to [46]

$$k_\mathrm{f} = A \cdot \mathrm{e}^{m_1\vartheta} \cdot \varphi^{m_2} \cdot \dot{\varphi}^{m_3} \cdot \mathrm{e}^{m_4/\varphi} \cdot (1+\varphi)^{m_5\vartheta+m_6} \cdot \mathrm{e}^{m_7\varphi} \cdot (1+\dot{\varphi})^{m_8\vartheta} \cdot \vartheta^{m_9}$$

A	m_1	m_2	m_3	m_4	m_5	m_6
2098.29	−0.002 72	0.223 12	0	-3×10^{-5}	0.000 28	0

m_7	m_8	m_9	ϑ	φ
−0.585 08	0.000 137	0	820 °C to 1200 °C	0.04 to 1.5

(b) Parameters for Generalized JMAK Model as in Equations 8 to 11 acc. to Hodgson and R. K. Gibbs [33]

Mechanism	Parameter	1	2	3	4	Q in kJ
Dynamic	a	5.60×10^{-4}	0	0.17	0.3	51.0
	b	5.60×10^{-4}	0	0.17	0.3	51.0
	c	1.60×10^{4}	0	−0.23	0	−69.0
Meta-Dynamic	a	0.00	0	0	0	0.0
	b	1.10	0	−0.8	0	−10.0
	c	2.60×10^{4}	0	−0.23	0	−69.0
Static	a	0.00	0	0	0	0.0
	b	2.30×10^{-15}	−2.5	0	1	230.0
	c	3.43×10^{2}	−0.5	0	0.4	−45.0

(c) Other Material Data and Model Coefficients

ϱ	c_p	α_Contact	$\alpha_\mathrm{Convection}$	ϵ_r
$\mathrm{kg\,m^{-3}}$	$\mathrm{J\,kg^{-1}\,K^{-1}}$	$\mathrm{W\,m^{-2}\,K^{-1}}$	$\mathrm{W\,m^{-2}\,K^{-1}}$	
7500.0	690.0	5000.0	10.0	0.8

Table 3: Descriptive Statistics and Weibull Distribution Parameters of Inter-Pass Durations

#	Data Mean	Data Std.	Data Min	Data Max	Dist. Shape α	Dist. Scale β	Dist. Mean	Dist. Std.
	s	s	s	s	1	s	s	s
R1-R2	6.633	1.471	5.115	15.955	8.212	6.543	6.170	0.893
R2-R3	4.435	0.995	3.040	11.100	7.706	4.408	4.143	0.637
R3-R4	5.988	2.193	4.015	21.000	7.030	5.623	5.261	0.881
R4-R5	5.655	0.471	4.745	7.115	13.800	5.711	5.500	0.487
R5-R6	5.045	0.567	3.635	6.030	8.707	5.276	4.989	0.684
R6-R7	5.196	0.589	4.235	8.095	16.115	5.085	4.921	0.376
R7-R8	6.436	1.557	4.705	13.170	8.147	6.161	5.807	0.847
R8-R9	6.081	0.723	4.745	8.260	14.631	5.901	5.694	0.477
R9-R10	7.008	0.775	5.260	9.215	11.127	7.140	6.822	0.742
R10-F1	9.233	0.399	8.290	10.385	37.736	9.203	9.069	0.303

Both are explained by the occurrence of outliers at large values, compare especially the passes R1–R2, R3–R4 and R7–R8, which have high empirical standard deviations and high maximum events.

3.2 Variational Behavior of the Rolling Process

The following questions shall be investigated and answered:

1. What is the difference in the behaviour of variations sourced in the input workpiece and arising within the process (manual handling)?
2. How can the variation of the input workpiece be efficiently depressed?
3. Or, similarly, how can the precision of the process be increased efficiently?
4. Is there a minimum number of passes needed to eliminate variations of the input workpiece?

For this, distinct simulations were carried out and compared with each other and the experimental data.

3.2.1 Different Sources of Variation

Two basic classes of variation sources can be identified in rolling processes, or, manufacturing processes in general: variations inherent to the input workpiece and variations arising in the regarded processes itself. Together with the variational behaviour of the process, these determine the variation of the resulting product. However, they presumably behave differently in the process. To investigate this, two simulations shall be carried out and compared. The first one only regards variations of the input workpiece and how they evolve during the process. The second one introduces additional variations within the process in means of varying inter-stand pause durations between the reversing passes. These originate, as denoted before, in the manual

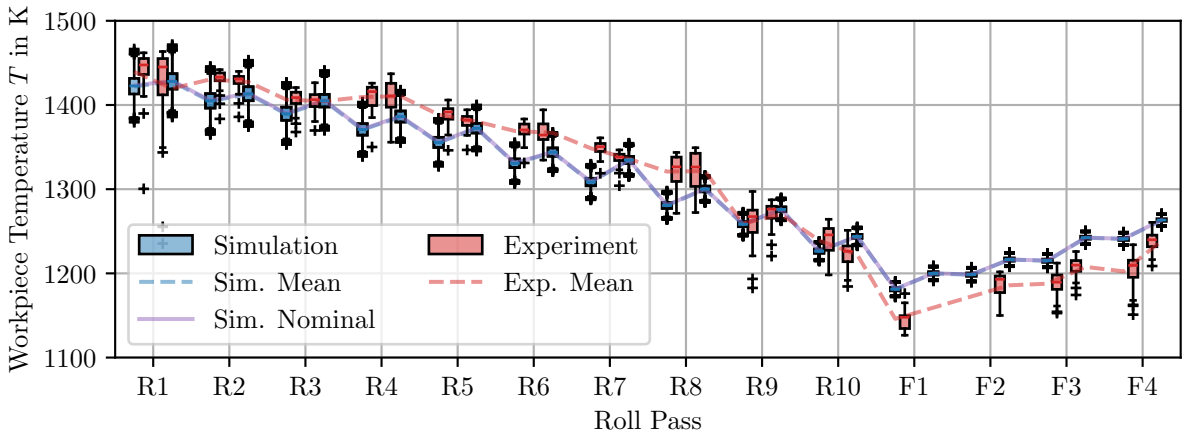

(a) Under Influence of Input Workpiece Variation

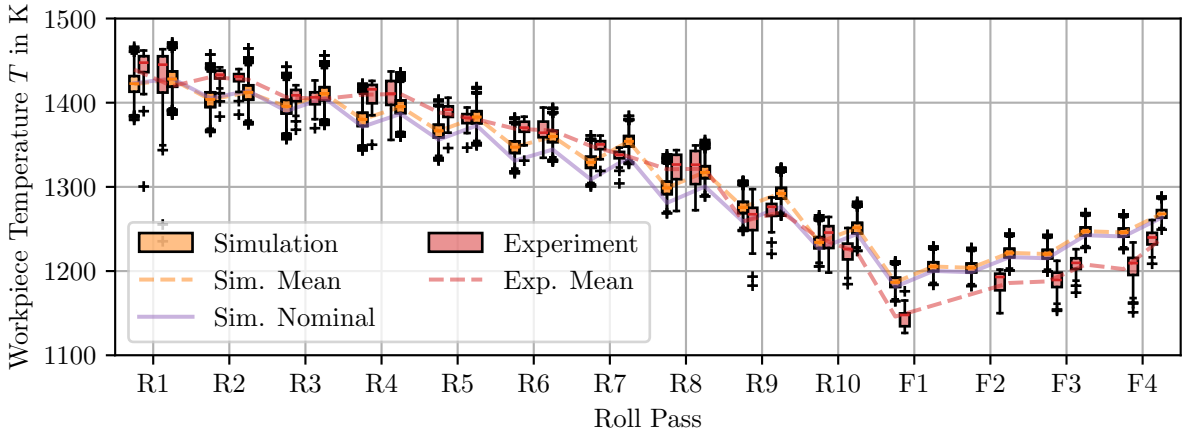

(b) Under Influence of Input Workpiece Variation and Pause Duration Variation

Figure 5: Variation of Workpiece Temperature

handling of the workpiece for feeding into the next pass. The focus of the following analysis lies on the temperature evolution of the workpiece, since this is crucial for microstructure evolution and final material properties, and will, presumably, be heavily effected by varying pause durations.

The temperature evolution of the first case is shown in Figure 5a. The uncertainty of the input workpiece was modelled using normal distributions for diameter and mean temperature, with expectation equal to the nominal value and relative standard deviations of 1 %. The box plots in the figure show the variation of the workpiece temperature, where the box marks the region from the lower to the upper quartile and the whiskers the distance of 1.5 of the inter-quartile-distance from the median. The variation of temperature decreases with each processing step and is remarkably small in the product. So there is something like a “natural” depression of variation in each process step.

The second case, however, is shown in Figure 5b. Here, the variation is not decreasing with each step, but increases in some of the transport steps. In contrast, roll passes still decrease the variation. If the overall variation decreases in the process depends on the ratio between the decrease in passes and the increase in transports. In this view, the goal of process design must

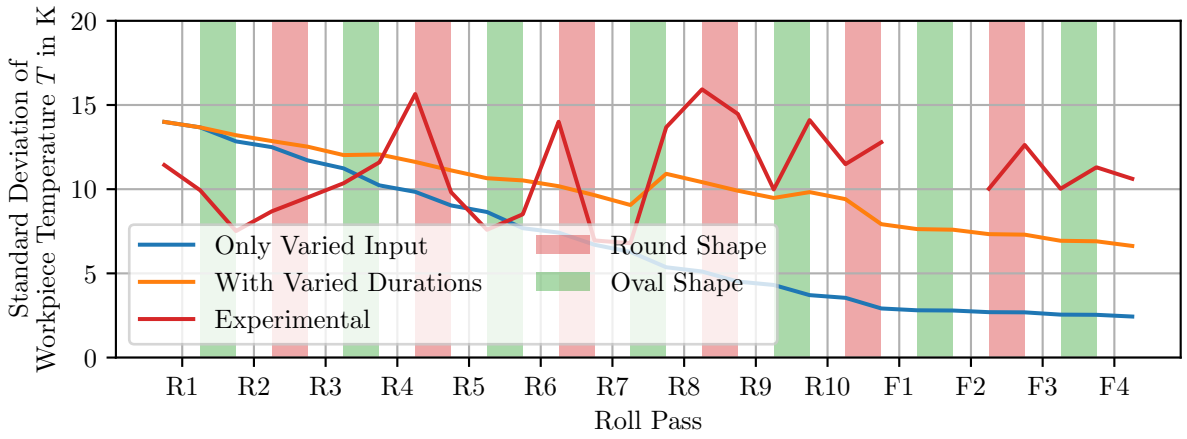

Figure 6: Comparison of Temperature Variation Evolution Between Input Variation and Process Variation

be to prevent an overall increase of variation in the process. The main vantage point for this is in our example to limit variation in pause durations.

Figure 6 shows the evolution of standard deviation in both cases in comparison, accompanied by the experimental results. One can see that the overall variation is increasing solely in reversing transports for the second case. Note that the influence of transports in oval cross-section shape is remarkably higher than those in round shape. This can be explained by the adverse surface-area-to-volume ratio of oval cross-sections.

The experimental results tendentiously show higher variations than proposed by the simulation, which is natural, since the simulation only regards selected sources of variation. Sometimes the pyrometer does not continuously hit the strand, which lowers the integral mean of the temperature signal. Therefore, values more than 30 K below of the median were dropped as outliers. However, there are several peaks in the experimental curve remarkably deviating from the simulation results. The gap in the data between F1 and F2 is due to the lack of a pyrometer there. Overall, the simulation including the pause durations gives a good first estimate of the workpiece temperature variation, although there seem to be further sources of variation missing.

As stated before, the actual workpiece temperature has significant influence on the microstructural processes happening within rolling and the pauses between the deformation steps. Figure 8 shows the variation of the mean grain size predicted by the simulation using only input variation in comparison to that using the pause duration variation. Note that the variation in grain size is significantly higher in the second case. A remarkable feature here is, that a prominent peak is occurring in the R10 pass, this is because the pass applies a deformation only slightly above the critical strain of recrystallization. The grain size deviation rises in the first pass from its certain initial value caused by the variation in temperature and draught. In reality, the mean grain size would also not be a certainly determined property because of differences in chemical composition and uncertainty of previous processes, especially the casting and reheating in the furnace. The final standard deviation, however, is predicted to be about 1 µm for the second case, which lies definitely within the measurement uncertainty of mean grain sizes from optical micrographs. So the variation of mean grain sizes can hardly be rated as significant for the current example. This statement may change if one regards local microstructural properties using more sophisticated models for temperature and microstructure evolution.

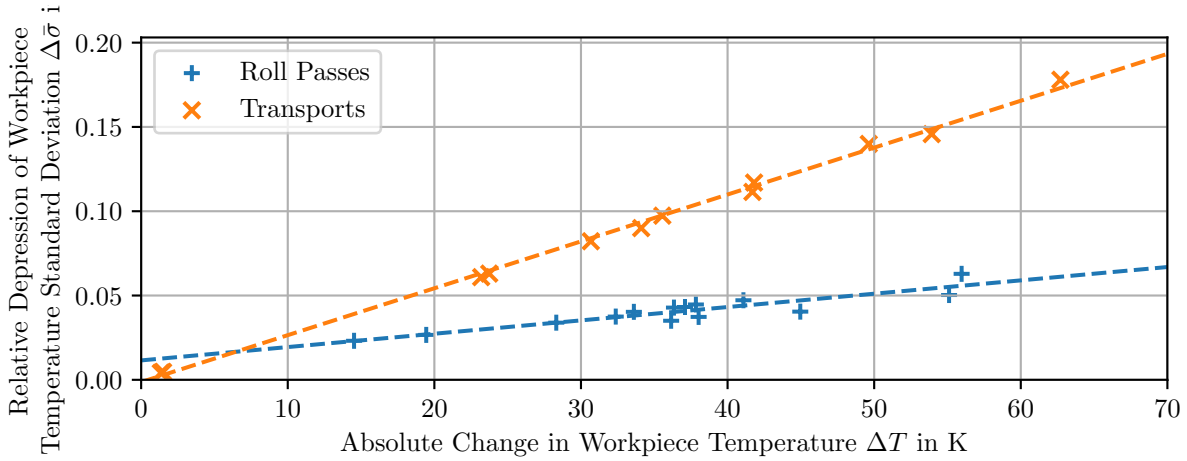

(a) Under Influence of Input Workpiece Variation

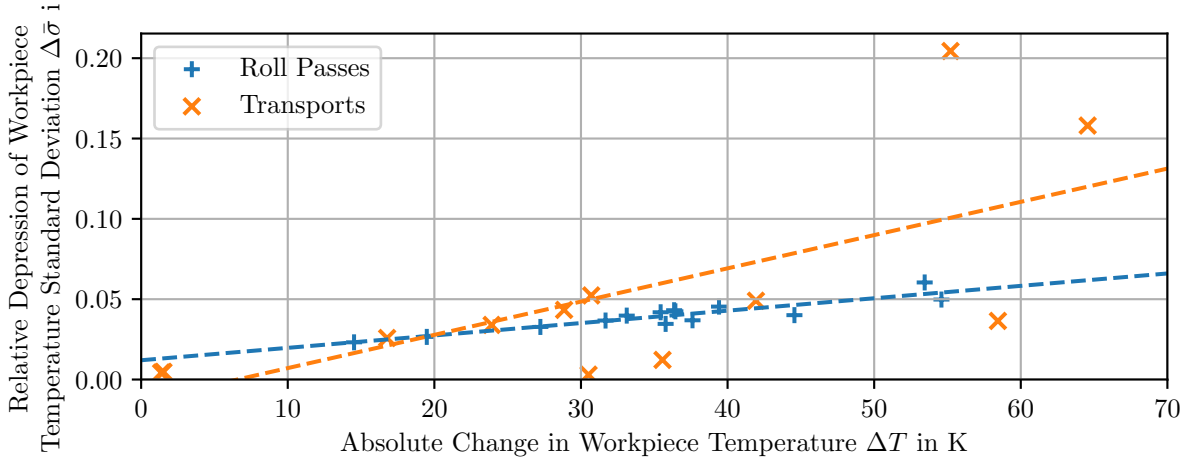

(b) Under Influence of Input Workpiece Variation and Pause Duration Variation

Figure 7: Correlation Between Change in Temperature Standard Deviation and Change in Temperature Per Unit

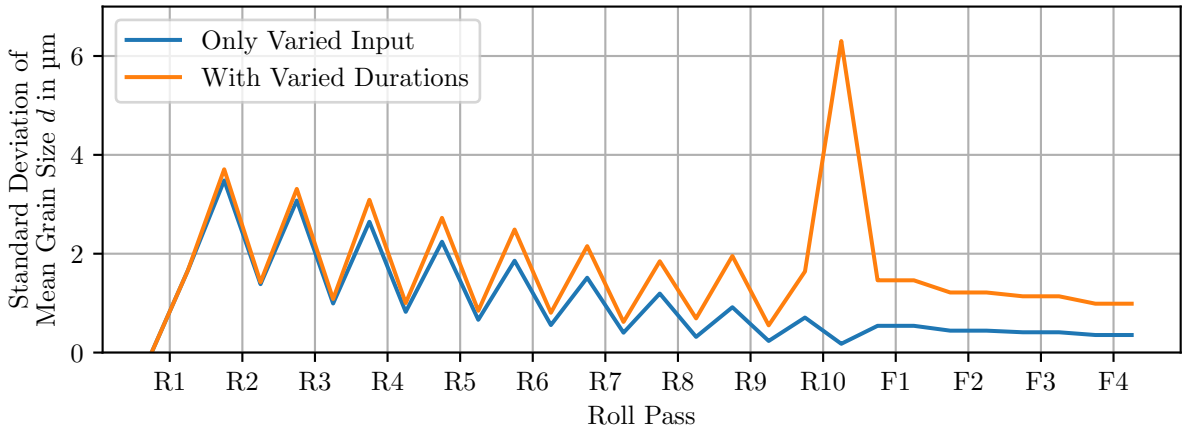

Figure 8: Comparison of Grain Size Variation Evolution Between Input Variation and Process Variation

3.2.2 Efficiency of Variation Depression in a Single Process Step

From the observation regarding the difference between oval and round shapes, the hypothesis can be stated that process steps with high influence on temperature have also high influence on the variation depression. This is proven by plotting the relative depression in standard deviation per step as in Equation 12 over the change in temperature in the step. This correlation can especially be observed in varying only the input workpiece as shown in Figure 7a, where the variation depressions in roll passes and transports show an approximately linear correlation to the temperature changes. In the case of varying pause durations, the roll passes still show the same behaviour, but the correlation in the transports is destroyed by the introduction of additional variation, as can be seen in Figure 7b. Nevertheless, it can be concluded that a process highly affecting a regarded property is also efficient in reducing the variation of this property introduced with the input workpiece, which seems plausible.

$$\Delta\bar{\sigma} = \frac{|\Delta\sigma|}{|\sigma|} \tag{12}$$

3.2.3 Elimination of Input Variation Along the Process Line

A common experiential statement found is that the variations in the input workpiece are eliminated after three to four passes. To validate this statement, simulations under different variations of the input workpiece have been carried out.

Figure 9a shows the depression of the filling ratio standard deviation along the pass sequence for different initial workpiece diameter variations. It is found that the variation decreases rapidly in the first three passes and is negligibly small in the fourth, no matter what initial variation was applied. So regarding the geometry, the validity of the former statement can be confirmed. Simulations using standard deviations higher than 5 % of the nominal value often failed in the current example. There was a significant probability for the workpiece to be too small, so gripping of the profile failed in the first or second pass (due to too few spread in the first).

Figure 9b, however, shows the depression of temperature variation along the pass sequence for different initial workpiece temperature variations. Although, the variation is effectively depressed

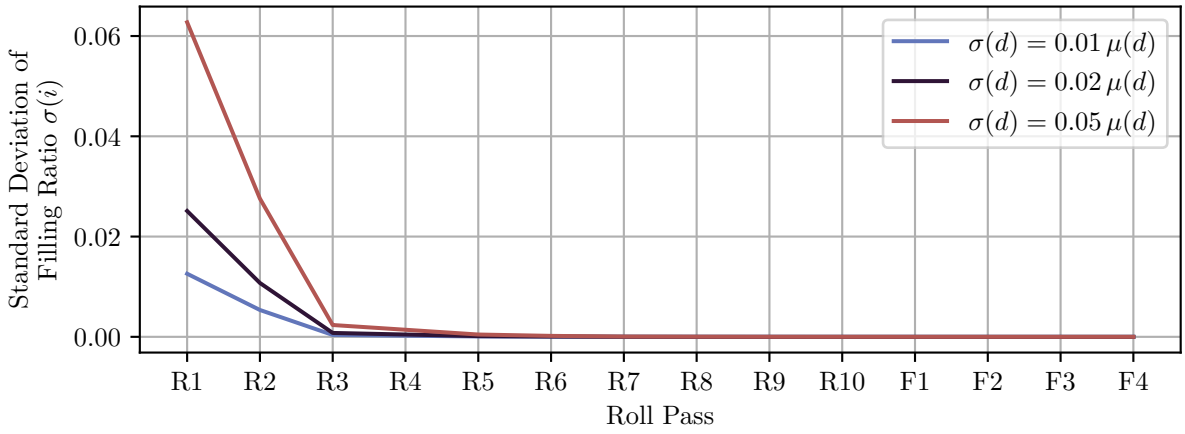

(a) Variation of Roll Pass Filling Ratios

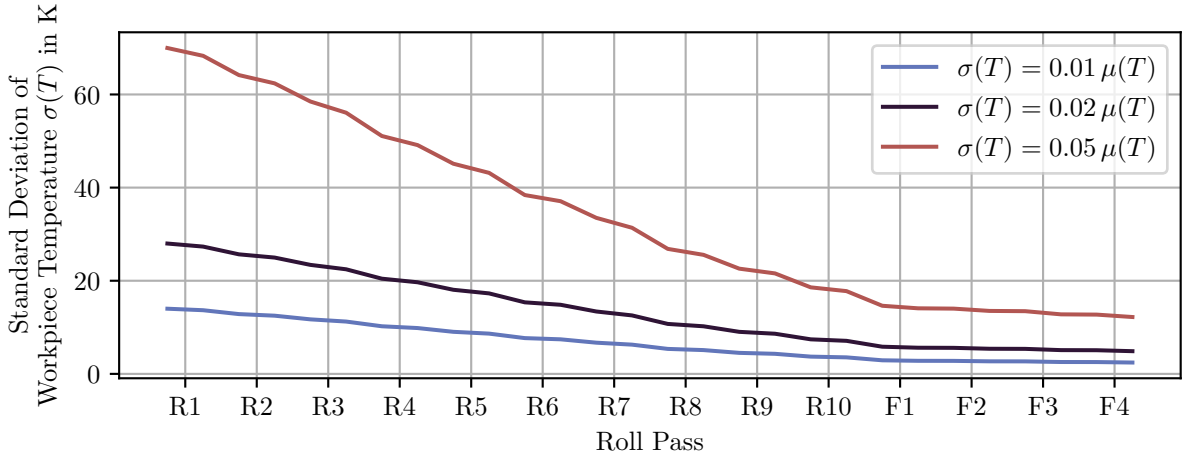

(b) Variation of Workpiece Temperature

Figure 9: Depression of Workpiece Variation

in the sequence, the variation of the output workpiece is still remarkably higher for higher input variations. So regarding the temperature evolutions, the statement can not be confirmed, especially in regard of microstructure evolution heavily affected by the temperature path taken.

4 Summary and Outlook

The method was found to give a good estimate of a rolling process' variational behaviour, however, dependent on the included influences and availability of statistical data that describe the input parameters. Uncertainties in input material were found to vanish along the process line, whereas uncertainties of the process itself were found to accumulate, which is in accordance with practical knowledge and intuition. A correlation was found between the size of the effect on a property, a process step applies, and its ability to depress already present uncertainties. Deviations in shape of the input workpiece were found to be equalized rapidly within a few passes. Deviations in temperature are reduced, but do not vanish. However, their actual impact on the microstructure was found to be negligible.

The method offers a general way to investigate a process regarding the evolution of deviations and their impact on product properties. More reliable and convincing result could be obtained by use of more detailed and sophisticated model approaches, however, at the cost of a significant increase in computational effort. Additional influences and sources of deviation can be included in the analysis easily, since all uncertain inputs are processed in parallel. For each of them, a reasonable estimate of their statistical distribution must be available from data or educated guessing.

References

[1] H. H. Ku. "Notes on the Use of Propagation of Error Formulas". In: *Journal of Research of the National Bureau of Standards, Section C: Engineering and Instrumentation* 70C.4 (Oct. 1966), p. 263. ISSN: 0022-4316. DOI: 10.6028/jres.070C.025. URL: https://nvlpubs.nist.gov/nistpubs/jres/70C/jresv70Cn4p263_A1b.pdf (visited on 04/12/2023).

[2] C. Lemieux. *Monte Carlo and Quasi-Monte Carlo Sampling*. Springer New York, 2009. ISBN: 978-0-387-78165-5. DOI: 10.1007/978-0-387-78165-5.

[3] C.-Y. Lin, W.-H. Huang, M.-C. Jeng, and J.-L. Doong. "Study of an Assembly Tolerance Allocation Model Based on Monte Carlo Simulation". In: *Journal of Materials Processing Technology* 70.1 (Oct. 1, 1997), pp. 9–16. ISSN: 0924-0136. DOI: 10.1016/S0924-0136(97)00034-4. URL: https://www.sciencedirect.com/science/article/pii/S0924013697000344 (visited on 12/02/2022).

[4] Zhengshu Shen, Gaurav Ameta, J. J. Shah, and J. K. Davidson. "A Comparative Study Of Tolerance Analysis Methods". In: *Journal of Computing and Information Science in Engineering* 5.3 (May 16, 2005), pp. 247–256. ISSN: 1530-9827. DOI: 10.1115/1.1979509. URL: https://doi.org/10.1115/1.1979509 (visited on 12/02/2022).

[5] J.-Y. Dantan and A.-J. Qureshi. "Worst-Case and Statistical Tolerance Analysis Based on Quantified Constraint Satisfaction Problems and Monte Carlo Simulation". In: *Computer-Aided Design* 41.1 (Jan. 2009), pp. 1–12. ISSN: 00104485. DOI: 10.1016/j.cad.2008.11.003. URL: https://linkinghub.elsevier.com/retrieve/pii/S0010448508002078 (visited on 09/30/2022).

[6] A.-J. Qureshi, J.-Y. Dantan, V. Sabri, P. Beaucaire, and N. Gayton. "A Statistical Tolerance Analysis Approach for Over-Constrained Mechanism Based on Optimization and Monte Carlo Simulation". In: *Computer-Aided Design* 44.2 (Feb. 1, 2012), pp. 132–142. ISSN: 0010-4485. DOI: 10.1016/j.cad.2011.10.004. URL: https://www.sciencedirect.com/science/article/pii/S0010448511002636 (visited on 12/02/2022).

[7] H. Yan, X. Wu, and J. Yang. "Application of Monte Carlo Method in Tolerance Analysis". In: *Procedia CIRP*. 13th CIRP Conference on Computer Aided Tolerancing 27 (Jan. 1, 2015), pp. 281–285. ISSN: 2212-8271. DOI: 10.1016/j.procir.2015.04.079. URL: https://www.sciencedirect.com/science/article/pii/S2212827115003418 (visited on 12/02/2022).

[8] C. Rausch, M. Nahangi, C. Haas, and W. Liang. "Monte Carlo Simulation for Tolerance Analysis in Prefabrication and Offsite Construction". In: *Automation in Construction* 103 (July 2019), pp. 300–314. ISSN: 09265805. DOI: 10.1016/j.autcon.2019.03.026. URL: https://linkinghub.elsevier.com/retrieve/pii/S092658051831121X (visited on 09/30/2022).

[9] M. Weiner, M. Schmidtchen, and U. Prahl. “A New Approach for Sintering Simulation of Irregularly Shaped Powder Particles – Part I: Model Development and Case Studies”. In: *Advanced Engineering Materials* (Feb. 2022). DOI: 10.1002/adem.202101513.

[10] M. Weiner, T. Zienert, M. Schmidtchen, J. Hubálková, C. G. Aneziris, and U. Prahl. “A New Approach for Sintering Simulation of Irregularly Shaped Powder Particles – Part II: Statistical Powder Modelling”. In: *Advanced Engineering Materials* (June 2022). DOI: 10.1002/adem.202200443.

[11] M. Weiner, C. Renzing, J. Mantel, M. Schmidtchen, and U. Prahl. *Supplemental Material for Rolling Process Variation Estimation Using a Monte-Carlo Method*. 2024. URL: https://github.com/pyroll-project/publication-weiner-variation.

[12] M. Weiner, Christoph Renzing, M. Stirl, M. Schmidtchen, and U. Prahl. “PyRolL - An Extensible OpenSource Framework for Rolling Simulation”. In: *Journal of Open Source Software* (2024).

[13] Max Weiner, Christoph Renzing, and Matthias Schmidtchen. *Pyroll-Project/Pyroll-Core: V2.1.0*. Version v2.1.0. Zenodo, Aug. 29, 2023. DOI: 10.5281/ZENODO.7817100. URL: https://zenodo.org/record/7817100 (visited on 09/28/2023).

[14] A. Hensel and T. Spittel. *Kraft- und Arbeitsbedarf bildsamer Formgebungsverfahren*. Leipzig: VEB Deutscher Verlag für Grundstoffindustrie, 1978.

[15] A. Hensel, P. Poluchin, and W. Poluchin. *Technologie der Metallformung*. 1st ed. Vol. 1. Leipzig: Deutscher Verlag für Grundstoffindustrie, 1990. ISBN: 3-342-00311-1.

[16] J. H. Hitchcock and W. Trinks. *Roll Neck Bearings*. Report of Special Research Committee on Roll Neck Bearings. New York: ASME, 1935, p. 51.

[17] A. E. Lendl. “Rolled Bars - Part I - Calculation of Spread between Non Parallel Roll Surfaces”. In: *Iron and Steel* 21.14 (1948), pp. 397–402.

[18] A. E. Lendl. “Rolled Bars - Part II - Application of Spread Calculation to Pass Design”. In: *Iron and Steel* 21.14 (1948), pp. 601–604. ISSN: 0021-1532.

[19] A. E. Lendl. “Rolled Bars - Part III - Application of Spread Calculation to Diamond Passes”. In: *Iron and Steel* 22.12 (1949), pp. 499–501. ISSN: 0021-1532.

[20] M. Weiner, Renzing, C., M. Stirl, and M. Schmidtchen. *PyRolL*. Version 1.0.5. Institute of Metal Forming, TU Bergakademie Freiberg. URL: https://pyroll-project.github.io.

[21] W. A. Johnson and R. F. Mehl. “Reaction Kinetics in Processes of Nucleation and Growth”. In: *Trans. Am. Inst. Min. Metall. Eng.* 135 (1939), pp. 416–458.

[22] Melvin Avrami. “Kinetics of Phase Change. I General Theory”. In: *The Journal of Chemical Physics* 7.12 (Dec. 1939), pp. 1103–1112. ISSN: 0021-9606, 1089-7690. DOI: 10.1063/1.1750380. URL: http://aip.scitation.org/doi/10.1063/1.1750380 (visited on 05/06/2022).

[23] Melvin Avrami. “Kinetics of Phase Change. II Transformation-Time Relations for Random Distribution of Nuclei”. In: *The Journal of Chemical Physics* 8.2 (Feb. 1, 1940), pp. 212–224. ISSN: 0021-9606, 1089-7690. DOI: 10.1063/1.1750631. URL: https://pubs.aip.org/jcp/article/8/2/212/215344/Kinetics-of-Phase-Change-II-Transformation-Time (visited on 01/22/2024).

[24] Melvin Avrami. “Granulation, Phase Change, and Microstructure Kinetics of Phase Change. III”. In: *The Journal of Chemical Physics* 9.2 (Feb. 1, 1941), pp. 177–184. ISSN: 0021-9606, 1089-7690. DOI: 10.1063/1.1750872. URL: https://pubs.aip.org/jcp/article/9/2/177/217869/Granulation-Phase-Change-and-Microstructure (visited on 01/22/2024).

[25] A. Kolmogorov. “ ”. In: 1.3 (1937), pp. 355–359.

[26] M. J. Luton and C. M. Sellars. “Dynamic Recrystallisation in Nickel and Nickel-Iron Alloys During High Temperature Deformation”. In: *Acta Metallurgica* 17 (1969), pp. 1033–1043.

[27] C. M. Sellars. “Recrystallization of Metals during Hot Deformation”. In: *Philosophical Transactions of the Royal Society of London. Series A, Mathematical and Physical Sciences* 288.1350 (Feb. 14, 1978), pp. 147–158. ISSN: 0080-4614, 2054-0272. DOI: 10.1098/rsta.1978.0010. URL: https://royalsocietypublishing.org/doi/10.1098/rsta.1978.0010 (visited on 01/22/2024).

[28] C. M. Sellars and J. A. Whiteman. “Recrystallization and Grain Growth in Hot Rolling”. In: *Metal Science* 13.3-4 (Mar. 1979), pp. 187–194. ISSN: 0306-3453. DOI: 10.1179/msc.1979.13.3-4.187. URL: http://www.tandfonline.com/doi/full/10.1179/msc.1979.13.3-4.187 (visited on 01/17/2024).

[29] C. M. Sellars. “The Kinetics of Softening Processes during Hot Working of Austenite”. In: *Czechoslovak Journal of Physics* 35.3 (Mar. 1985), pp. 239–248. ISSN: 0011-4626, 1572-9486. DOI: 10.1007/BF01605090. URL: http://link.springer.com/10.1007/BF01605090 (visited on 02/12/2024).

[30] John H. Beynon and C. Michael Sellars. “Modelling Microstructure and Its Effects during Multipass Hot Rolling.” In: *ISIJ International* 32.3 (1992), pp. 359–367. ISSN: 0915-1559. DOI: 10.2355/isijinternational.32.359. URL: http://www.jstage.jst.go.jp/article/isijinternational1989/32/3/32_3_359/_article (visited on 01/17/2024).

[31] G. Glover and Cm. Sellars. “Static Recrystallization after Hot Deformation of Iron”. In: *Metallurgical Transactions* 3.8 (Aug. 1972), pp. 2271–2280. ISSN: 0026-086X, 2379-0083. DOI: 10.1007/BF02643242. URL: https://link.springer.com/10.1007/BF02643242 (visited on 01/22/2024).

[32] G. Glover and C. M. Sellars. “Recovery and Recrystallization during High Temperature Deformation of -Iron”. In: *Metallurgical Transactions* 4.3 (Mar. 1973), pp. 765–775. ISSN: 0026-086X, 2379-0083. DOI: 10.1007/BF02643086. URL: https://link.springer.com/10.1007/BF02643086 (visited on 01/22/2024).

[33] P. D. Hodgson and R. K. Gibbs. “A Mathematical Model to Predict the Mechanical Properties of Hot Rolled C-Mn and Microalloyed Steels.” In: *ISIJ International* 32.12 (1992), pp. 1329–1338. ISSN: 0915-1559. DOI: 10.2355/isijinternational.32.1329. URL: http://www.jstage.jst.go.jp/article/isijinternational1989/32/12/32_12_1329/_article (visited on 01/17/2024).

[34] A. Laasraoui and J. J. Jonas. “Prediction of Temperature Distribution, Flow Stress and Microstructure during the Multipass Hot Rolling of Steel Plate and Strip.” In: *ISIJ International* 31.1 (1991), pp. 95–105. ISSN: 0915-1559. DOI: 10.2355/isijinternational.31.95. URL: http://www.jstage.jst.go.jp/article/isijinternational1989/31/1/31_1_95/_article (visited on 01/17/2024).

[35] A. Laasraoui and J. J. Jonas. "Recrystallization of Austenite after Deformation at High Temperatures and Strain RatesAnalysis and Modeling". In: *Metallurgical Transactions A* 22.1 (Jan. 1991), pp. 151–160. ISSN: 0360-2133, 2379-0180. DOI: 10.1007/BF03350957. URL: https://link.springer.com/10.1007/BF03350957 (visited on 01/31/2024).

[36] C.A. Hernandez, S.F. Medina, and J. Ruiz. "Modelling Austenite Flow Curves in Low Alloy and Microalloyed Steels". In: *Acta Materialia* 44.1 (Jan. 1996), pp. 155–163. ISSN: 13596454. DOI: 10.1016/1359-6454(95)00153-4. URL: https://linkinghub.elsevier.com/retrieve/pii/1359645495001534 (visited on 01/22/2024).

[37] S.F. Medina and C.A. Hernandez. "Modelling of the Dynamic Recrystallization of Austenite in Low Alloy and Microalloyed Steels". In: *Acta Materialia* 44.1 (Jan. 1996), pp. 165–171. ISSN: 13596454. DOI: 10.1016/1359-6454(95)00154-6. URL: https://linkinghub.elsevier.com/retrieve/pii/1359645495001546 (visited on 02/12/2024).

[38] A. I. Fernández, P. Uranga, B. López, and J. M. Rodriguez-Ibabe. "Static Recrystallization Behaviour of a Wide Range of Austenite Grain Sizes in Microalloyed Steels." In: *ISIJ International* 40.9 (2000), pp. 893–901. ISSN: 0915-1559. DOI: 10.2355/isijinternational.40.893. URL: http://www.jstage.jst.go.jp/article/isijinternational1989/40/9/40_9_893/_article (visited on 02/12/2024).

[39] A Fernandez, P Uranga, B Lopez, and J Rodriguezibabe. "Dynamic Recrystallization Behavior Covering a Wide Austenite Grain Size Range in Nb and NbTi Microalloyed Steels". In: *Materials Science and Engineering A* 361.1-2 (Nov. 25, 2003), pp. 367–376. ISSN: 09215093. DOI: 10.1016/S0921-5093(03)00562-8. URL: https://linkinghub.elsevier.com/retrieve/pii/S0921509303005628 (visited on 02/12/2024).

[40] Kai Karhausen and Reiner Kopp. "Model for Integrated Process and Microstructure Simulation in Hot Forming". In: *Steel Research* 63.6 (June 1992), pp. 247–256. ISSN: 01774832. DOI: 10.1002/srin.199200509. URL: https://onlinelibrary.wiley.com/doi/10.1002/srin.199200509 (visited on 01/22/2024).

[41] W. Roberts, H. Boden, and B. Ahlblom. "Dynamic Recrystallization Kinetics". In: *Metal Science* 13.3-4 (Mar. 1979), pp. 195–205. ISSN: 0306-3453. DOI: 10.1179/msc.1979.13.3-4.195. URL: http://www.tandfonline.com/doi/full/10.1179/msc.1979.13.3-4.195 (visited on 01/22/2024).

[42] T. M. Maccagno, J. J. Jonas, and P. D. Hodgson. "Spreadsheet Modelling of Grain Size Evolution during Rod Rolling." In: *ISIJ International* 36.6 (1996), pp. 720–728. ISSN: 0915-1559. DOI: 10.2355/isijinternational.36.720. URL: http://www.jstage.jst.go.jp/article/isijinternational1989/36/6/36_6_720/_article (visited on 01/17/2024).

[43] Fulvio Siciliano and John J. Jonas. "Mathematical Modeling of the Hot Strip Rolling of Microalloyed Nb, Multiply-Alloyed Cr-Mo, and Plain C-Mn Steels". In: *Metallurgical and Materials Transactions A* 31.2 (Feb. 2000), pp. 511–530. ISSN: 1073-5623, 1543-1940. DOI: 10.1007/s11661-000-0287-8. URL: https://link.springer.com/10.1007/s11661-000-0287-8 (visited on 01/17/2024).

[44] C. Zener and J. H. Hollomon. "Effect of Strain Rate Upon Plastic Flow of Steel". In: *Journal of Applied Physics* 15.1 (Jan. 1944), pp. 22–32. ISSN: 0021-8979, 1089-7550. DOI: 10.1063/1.1707363. URL: http://aip.scitation.org/doi/10.1063/1.1707363 (visited on 05/06/2022).

[45] M. Weiner, Mantel, J., and M. Schmidtchen. *PyRolL JMAK Recrystallization*. Version 2.2.0. Institute of Metal Forming, TU Bergakademie Freiberg. URL: https://github.com/pyroll-project/pyroll-jmak-recrystallization.

[46] M. Spittel and T. Spittel. "Steel Symbol/Number: C45/1.0503". In: *Metal Forming Data of Ferrous Alloys - Deformation Behaviour*. Ed. by H. Warlimont. Red. by W. Martienssen. Vol. 2C1. Berlin, Heidelberg: Springer Berlin Heidelberg, 2009, pp. 210–215. ISBN: 978-3-540-44758-0 978-3-540-44760-3. DOI: 10.1007/978-3-540-44760-3_26. URL: http://materials.springer.com/lb/docs/sm_lbs_978-3-540-44760-3_26 (visited on 04/25/2023).